Title: Quantitative Analysis of Fiber Tractography in Cervical Spondylotic Myelopathy

Running Title: Fiber Tractography and CSM

Chun-Yi Wen [#], Jiao-Long Cui [#], Lee Man Pan, Kin-Cheung Mak, and Keith Dip-Kei. Luk, Yong Hu [*]

Department of Orthopaedics and Traumatology, Li Ka Shing Faculty of Medicine, The University of Hong Kong

"[#]" Equally contribution to this manuscript

"*****" Corresponding Author

Dr. Yong Hu

Dept. of Orthopaedics and Traumatology,

The University of Hong Kong

Address: 12 Sandy Bay Road, Pokfulam, Hong Kong

Email addressyhud@hku.hk

Tel: (852) 29740336; Fax: (852) 29740335

Acknowledgements

The authors would like to thank the support from the General Research Fund from The University Grant Council of Hong Kong (771608M/774211M). The authors would like to thank Prof EX Wu, Drs. Henry Mak and Q Chan for their assistant in MRI scanning.

Abstract

BACKGROUND AND CONTEXT: Diffusion tensor fiber tractography is an emerging tool for visualization of spinal cord microstructure. However, there are few quantitative analyses of the damage in the nerve fiber tracts of the myelopathic spinal cord.

PURPOSE The aim of this study was to develop a quantitative approach for fiber tractography analysis in cervical spondylotic myelopathy (CSM).

STUDY DESIGN/SETTING: Prospective study on a series patients.

MATERIALS AND METHODS A total of 22 volunteers were recruited with informed consent, including 15 healthy subjects and 7 CSM patients. The clinical severity of CSM was evaluated using modified JOA score. The microstructure of myelopathic cervical cord wee analyzed using diffusion tensor imaging (DTI). DTI was performed with a 3.0-Tesla MRI scanner using pulsed gradient, spin-echo-echo-planar imaging (SE-EPI) sequence. Fiber tractography was generated via TrackVis with fractional anisotropy threshold set at 0.2 and angle threshold at 40 degree. Region of interest (ROI) was defined to cover C4 level only or the whole-length cervical spinal cord from C1 to C7 for analysis. The length and density of tracked nerve bundles were measured for comparison between healthy subjects and CSM patients.

RESULTS The length of tracked nerve bundles significantly shortened in CSM patients as compared with healthy subjects (healthy: 6.85-77.90 mm; CSM: 0.68-62.53 mm). The density of the tracked nerve bundles was also lower in CSM patients (healthy: 086±0.03, CSM: 0.80±

0.06, p<0.05). Although the definition of ROI covering C4 only or whole cervical cord appeared not to affect the trend of the disparity between healthy and myelopathic cervical cords, the density of the tracked nerve bundle through whole myelopathic cords was in an association with the modified JOA score in CSM cases (r=0.949, p=0.015), yet not found with ROI at C4 only (r=0.316, p=0.684).

CONCLUSION The quantitative analysis of fiber tractography is a reliable approach to detect cervical spondylotic myelopathic lesions compared to healthy spinal cords. It could be employed to delineate the severity of CSM.

Key words: Diffusion tensor imaging, Fiber tractography, Cervical spondylotic myelopathy, Spinal cord.

Introduction

Cervical spondylotic myelopathy (CSM) is the most common type of spinal cord dysfunction in patients older than 55 years [1-3]. However, the exact pathophysiology of CSM remains poorly understood. The natural history of CSM is known to be associated with the enclosure of thespinal cord in a narrowed canal as a result of degenerative disc and spondylosis [4]. Nevertheless, the severity of the spinal cord compression does not necessarily correlate with the signs and symptoms of CSM patients [5-7]. For example, cases with significant cord compression may not exhibit any neurological signs, while cases with mild compression of the cord may develop neurological signs [4, 8]. Thus, the changes in gross morphology of the spinal cord as revealed by anatomical magnetic resonance imaging (T1-weighted or T2-weighted images) may not reflect the exact pathophysiological changes in spinal cord [4].

There is growing interest in the use of diffusion tensor imaging (DTI) and fiber tractography (FT) as imaging tools for evaluation of the microstructural changes in spinal cord trauma and degeneration [9-20]. All such studies have reported a decrease in fractional anisotropy (FA) of injured or degenerated spinal cord. FA is a commonly used parameter derived from the eigenvalues of the diffusion matrix [21]; however, eigenvector data have not been reported. As the principal eigenvector tends to be parallel with the orientation of white matter fiber bundles, fiber tractography can be generated through integration of three-dimensional white matter trajectories based on the principal diffusion directions [22].

The advantage of fiber tractography is that it provides integrated eigenvalue and eigenvector data of the diffusion matrix. Several studies [14, 18] have applied visual assessment of FT and proposed its prognostic value in CSM. However, it is mainly used as a visualization tool for evaluation of spinal cord lesions [18, 23-26].

In validation experiments, microstructural data from fiber tractography images were compared with histological details [27], providing a foundation for the potential clinical application of quantitative FT analysis of the spinal cord. Quantitative FT analysis was recently performed in an attempt to correlate with clinical findings in patients with acute spinal cord injury [28]. However, to our knowledge there are no studies examining quantitative FT analysis in CSM, a chronically compressive spinal cord injury.

Recently, the quantitative FT analysis was proposed to evaluate chronic compressive spinal cord lesion, i.e. CSM [18, 19]. There was no agreement yet on the selection of ROI and morphometric parameters in the quantitative FT analyses for CSM patients. As previous reported, the maximal compression level (MCL) at Sagittal T2 images of myelopathic cord was chosen as ROI, while C2 as a reference [19]. The ratio of tracked nerve bundles at MCL over C2 was measured to correlate the prognosis of CSM after surgical decompression. In another study, fiber tractography was performed at the selected level as well as C1 and C7. Only the pattern of fiber tractography was described to correlate the status of neurological deficit in CSM patients [18]. In this study, we aimed to (1) develop a quantitative FT analysis

approach to delineate myelopathic lesions and to correlate it with clinical severity of CSM, and then (2) investigate the influence of ROI selection and curvature of cervical cord on the results of FT analyses.

Materials and Methods

Subjects

The institutional review board of research ethics approved all experimental procedures in this study. All volunteers were screened to confirm their eligibility. The inclusion criteria for healthy subjects were those having intact sensory and motor function evaluated, and negative Hoffman's sign under physical examination. Subjects having any neurological signs and symptoms or any past history of neurological injury, disease, or operations were excluded. CSM patients were recruited in authors' institute. Experienced spine surgeons made a clinical diagnosis of CSM based on the patient's symptoms and signs, as well as radiological findings. The neurological deficits of CSM patients were systemically evaluated using the Japanese Orthopaedic Association (JOA) scoring system. The demographic, clinical, radiological and electrophysiological characteristics of CSM patients were listed in Table 1, which unveiled the extent of cervical cord involved and the severity of neurological functional impairment.

MRI Scanning

All images were taken via a 3.0 Tesla MRI scanner (Philips Achieva, Best, the Netherlands). Pulse sequence programming was performed prior to scanning to optimize the image quality. During the acquisition process, the subject was placed in a supine position with the sense neuro-vascular (SNV) head and neck coil enclosing the cervical region, and was instructed not to swallow to minimize motion artifacts. The subject was then scanned with

anatomical T1-weighted (T1W) and T2-weighted (T2W) images, as well as by diffusion tensor images (DTI).

Sagittal and axial T1W and T2W images were acquired for each subject. A fast spin echo (FSE) sequence was employed. For sagittal imaging, the imaging parameters were as follows: field of view (FOV) = 250×250 mm, slice thickness = 3 mm, slice gap = 0.3 mm, fold-over direction = Feet/Head (FH), number of excitations (NEX) = 2, resolution = 0.92×1.16×3.0 mm^3 (T1W) and 0.78×1.01×3.0 mm^3 (T2W), recon resolution = 0.49×0.49×3.0 mm^3, and time of echo (TE) / time of repetition (TR) = 7.2 / 530 ms (T1W) and 120 / 3314 ms (T2W). A total of 11 sagittal images covering the whole cervical spinal cord were acquired. For axial imaging, the imaging parameters were as follow: FOV =80×80 mm, slice thickness = 7 mm, slice gap = 2.2 mm, fold-over direction = anterior/posterior (AP), NEX = 3, resolution = 0.63×0.68×7.0 mm^3 (T1W) and 0.63×0.67×7.0 mm^3 (T2W), recon resolution = 0.56×0.55×3.0 mm^3 (T1W) and 0.63×0.63×7.0 mm^3 (T2W), and TE / TR = 8 / 1000 ms (T1W) and 120 / 4000 ms (T2W). Cardiac vectorcardiogram (VCG) triggering was applied to minimize the pulsation artifact from CSF.

A total of 12 axial images covering the whole cervical spinal cord from C1 to C7 were acquired. Diffusion MRI images were acquired using pulsed sequences: single-shot spin-echo echo-planar imaging (SE-EPI). Diffusion encoding was in 15 non-collinear and non-coplanar diffusion directions with a b-value = 600 s/mm^2. The imaging parameters were as follows: FOV = 80×80 mm, slice thickness = 7 mm, slice gap = 2.2 mm, fold-over direction = AP, NEX = 3, resolution = 1.00×1.26×7.0 mm^3, recon resolution = 0.63×0.64×7.0 mm^3, and TE / TR = 60 ms / 5 heartbeats. The image slice planning was the same as the anatomical axial T1W and T2W images, with 12 slices covering the cervical spinal cord from C1 to C7. The average duration of diffusion tensor imaging (DTI) was 24 min per subject, with an average heart rate of 60 beats per min. Spatial saturation with Spectral Presaturation with Inversion Recovery (SPIR) was applied to suppress the fold-over effect. To alleviate the EPI distortion

problem caused by increased magnetic susceptibility at 3.0 T, the distortion correction method based on the reversed gradient polarity and parallel imaging was employed [29-31].

Post-processing of Diffusion Tensor Fiber Tractography

Fiber tractography was generated via Diffusion Toolkit v0.6 with interpolated streamline algorithm and visualized using TrackVis v 0.6 (**www.trackvis.org**, Harvard Medical School, Boston, MA, USA). The threshold for fiber tracking termination was set at a voxel with the fractional anisotropy value lower than 0.20 and/or the angle of principal eigenvectors larger than 40 degree. The region of interests (ROIs) was defined to cover the whole length of the cervical spinal cord from C1 to C7 or C4 only (Fig.1.). The ROIs were drawn manually to cover whole spinal cord with the reference to the b0 image [32]. The track and voxel count, and the length of tracked fiber in ROIs were automatically calculated via the built-in program of TrackVis. The density of tracked fibers was calculated as the ratio of the track over the voxel count in the ROIs. The length of the tracked fiber indicated the fiber connectivity. Fractional anisotropy (FA) and the trace values (sum of diffusivities) of healthy and myelopathic spinal cord were also measured accordingly [32, 33].

Measurement of Spine Cord Curvature

The measurement of spinal cord curvature was performed on T2W sagittal images using Image J (National Institute of Health, Bethesda, MD, USA). A total of seven lines were drawn parallel to the intervertebral discs from C1/2 to C7/T1. The angles formed between the line at C4/5 and the other disc levels were measured, and the summation of the angles showed the curvature of the cervical spine column as an indicator of spinal cord curvature (Fig. 2). The healthy spinal cords were categorized as straight (HS) or curved (HC) based on their curvature below or above the average angle.

Statistical Analysis

Comparisons of FA, trace, the track or voxel count, fiber density, and fiber length were performed between healthy and CSM patients using the student *t* test. The Spearman correlation was conducted to analyze the link between clinical and DTI findings. Further analyses were performed after classification by healthy spinal cord curvature using one-way ANOVA and *post-hoc* test. The level of significance was set at $p<0.05$.All data analyses were performed using SPSS 15.0 analysis software (SPSS Inc, Chicago, IL, USA).

Results

A total of 22 volunteers, including 15 adult healthy subjects (42±6 years old) and 7 CSM patients (56±10 years old), met with the inclusive criteria and were recruited in this study. As well as presenting with lower JOA scores (CSM: 10±2 *vs* full score: 17), CSM patients showed a decrease in FA (healthy: 0.67±0.08 *vs.* CSM: 0.56±0.10) and an increase trace values (sum of diffusivities) (healthy: 3.21±0.22*E-03 *vs.* CSM: 4.42±1.15*E-03). Fiber tractography also revealed that the tracked fibers were loosely organized in myelopathic spinal cords, with short or disoriented fibers (Fig. 3), when compared to normal spinal cords.

Influence of ROI definition on parameters of quantitative fiber tractography

For both the healthy and the CSM groups, the track count and voxel count in fiber tractography were significantly higher when the ROI was set C1 to C7 as compared with the ROI at C4 only (Track Count – healthy: C4 1187.40±442.06 *vs.* C1-C7 3064.40±482.38; CSM: C4 367.43±125.32 *vs.* C1-C7 2282.71±293.80; Voxel Count – healthy: C4 1727.47±521.81 *vs.* C1-C7 3564.33±526.65; CSM: C4 702.57±232.43 *vs.* C1-C7 2860.71±487.76). Further, there was a significant difference in both track and voxel count between the healthy and CSM group regardless of ROIs definition at either C1 to C7 or C4 only (Track Count – C4: p=0.0001, C1-C7: p=0.0008; Voxel Count: C4: p=0.0001, C1-C7:

p=0.0074) (Fig. 4a-b).

For both the healthy and the CSM groups, the densities of the tracked fibers were also significantly higher when the ROI was set C1 to C7 as compared with the ROI at C4 only (healthy: C4 0.68±0.07 *vs.* C1-C7 086±0.03; CSM: C4 0.53±0.07 *vs.* C1-C7 0.80±0.06). Further, there was a significant difference in the densities of the tracked fibers between the healthy and CSM group regardless of ROIs definition at either C1 to C7 or C4 only (C4: p=0.0001, C1-C7: p=0.0064) (Fig. 4c).

The length of tracked fibers was reduced when changing the ROI from C4 only to the whole length of spinal cord (from C1 to C7) (healthy: C4 43.09±16.65 *vs.* C1-C7 27.11±18.33 mm; CSM: C4 25.67±8.36 *vs.* C1-C7 17.30±6.06 mm) (Fig. 4d). The length of fiber track was significantly shorter in CSM patients compared with healthy subjects (C4: p=0.0012, C1-C7: p=0.0088). The distribution of the length of the tracked fiber is shown in Figure 5. The long fiber tracks were obviously lost in CSM (healthy: C4 1.95-76.68 *vs.* C1-C7 6.85-77.90 mm; CSM: 0.68-57.91 *vs.* C1-C7 0.68-62.53 mm).

Although the definition of ROI covering C4 only or whole cervical cord appeared not to affect the trend of the disparity between healthy and myelopathic cervical cords, the density of the tracked nerve bundle through whole myelopathic cords was in an association with the modified JOA score in CSM cases (r=0.949, p=0.015), yet not found with ROI at C4 only (r=0.316, p=0.684).

Influence of spinal cord curvature on parameters of quantitative fiber tractography

There was an obvious difference in the curvature of the cervical spine between individuals observed when placing for MRI scanning. The average angle for the curvature of the cervical spine was 20.4° in healthy subjects. A total of six healthy subjects had a ‘straight’ spinal cord (HS group), ranging from 10.1° to 18.5°, while nine healthy subjects had a ‘curved’ spinal cord (HC), ranging from 20.4° to 30.4°. The mean curvature of myelopathic

spinal cord was 43.6°, ranging from 42.4° to 44.47°. In the ROI from C1 to C7, the track and voxel count was significantly lower in the curved compared with the straight spinal cord (Track count – HS: 3236.33±537.23 *vs.* HC: 2805.38±813.26; Voxel count – HS: 3730.17±525.04 *vs.* HC: 3295.02±995.32). In comparison with the straight or curved healthy spinal cord, both track and voxel count were decrease in CSM (Track count: HS *vs.* CSM, p=0.002; HC *vs.* CSM, p=0.003; Voxel count: HS *vs.* CSM, p=0.01; HC *vs.* CSM, p=0.03) (Fig. 6a-b).

There was no significant effect of spinal cord curvature on the density and length of the tracked fibers (HS: 30.33±8.69 *vs.* HC: 25.32±8.77). There was a marginal difference detected in the density under the sub-group analysis according to the curvature of spinal cord (HS *vs.* CM, p=0.046; HC *vs.* CM, p=0.054) (Fig. 6c). The length of the fiber track remained lower in the CSM than in healthy subjects regardless of presence of a straight or curved spinal cord (HS *vs.* CSM, p=0.001; HC *vs.* CSM, C1-C7, p=0.028) (Fig. 6d).

Discussion and Conclusion

Cervical spondylotic myelopathy is a clinical diagnosis based on the description of a chronic compression of spinal cord in a stenotic canal as a result of spondylosis and/or disc degeneration with subsequent neurological deficit [1]. However, the wide range of clinical signs and symptoms and non-specific information of anatomical MRI have made it difficult to make a precise diagnosis of CSM (e.g., the delineation of the extent or severity of myelopathic lesion) [1]. In the present study, using diffusion tensor fiber tractography, we developed a direct quantitative approach to quantify the organization and connectivity of fiber bundles in the spinal cord in the living human body in a non-invasive manner. We found that quantitative analysis of fiber tractography (FT) could reliably detect the microstructural difference between healthy and myelopathic spinal cord, regardless of ROI selection and spinal cord curvature. Importantly, we used the fiber length parameter to indicate the

connectivity of fiber bundles in the spinal cord, which was sensitive for detection of poor fiber bundle organization in CSM. By contrast, fiber density exhibited poor sensitivity. The poor fiber organization in CSM was reflected by a decrease in FA and an increase in diffusivity .

Chang Y *et al*. previously examined the number of passing fibers in the spinal cord in cases of cervical spinal cord trauma using a C4 level ROI [28]. Recently, the quantitative FT analyses were also employed in CSM cases [18, 19]. However, the selection of ROI and parameters varied among these studies. The maximal compression level of myelopathic cervical cord was chosen with C2 as a reference to calculate the ratio of tracks in fiber tractography [19]. In the other study, the selected level was analyzed with C1 and C7 as the reference [18]. Importantly, the prognostic value of quantitative FT analyses was implied in surgical management of CSM patients. It was shown that the ratio or pattern of tracked nerve fibers appeared to correlate with the postoperative improvement of CSM patients after surgical decompression. However, they did not examine the influence of ROI selection on the outcome of the quantitative FT analysis. As shown in the present study, ROI selection can influence the exact values generated from quantitative FT analysis. For example, the track and voxel count and the density of tracked fibers were higher when the whole length spinal cord was selected rather than the C4 level only. Although this did not change the trend of CSM-related changes, the three-dimensional image of fiber tractography with the C1 to C7 ROI selection was more close to the actual volume and structure of the spinal cord (Fig.1). Importantly, we found that the density of tracked nerve bundles correlated well with the clinical severity of CSM when the myelopathic cervical cord from C1 to C7 was analyzed as a whole. Our findings suggested that the ROI from C1 to C7 should be taken, rather than MCL only, to reflect the overall status of myelopathic cervical cord.

We also explored the influence of the curvature of the spinal cord on FT analysis, and found that spinal cord curvature did not alter the trend of CSM-related changes. However, the

data from subjects with a curved spinal cord exhibited a large variation, and analyses failed to detect a significant difference in the fiber density between healthy and myelopathic spinal cord after taking spinal cord curvature into consideration, particularly when choosing C1-7 as an ROI. Nevertheless, we did detect a statistically significant difference in the parameters of FT analysis (i.e., length of tracked fibers). A recent report used the fiber tract (FT) ratio as a quantitative assessment of the spinal cord, and found a significant correlation with the recovery rates in CSM patients [19]. However, in that study the FT ratio did not reflect the severity of neurological deficit.

We found that the track count (i.e., the number of fiber projections) and the voxel count (i.e., the number of voxels) that passed through the tracked fibers in the ROIs were significantly lower in the injured spinal cord as compared with the healthy spinal cord. This may be explained by reduction in the seed points for fiber bundles from the basic principle of fiber tractography [34]. As each seed point was screened by the values of FA, the low FA in CSM indicated loss of anisotropy of the diffusion ellipsoid of water molecules, as previously reported [9-17]. As such, less water molecules could be used as the seed points for the subsequent fiber tracking, resulting in loss of track count and track density. The length of the tracked fibers was statistically different between healthy and diseased groups. Although the tracking did not originate from the actual anatomical structure of the nerve bundles in the spinal cord, these data indicate a continuity of intact nerve fibers, as the anisotropy of water molecules occurs preferentially along the fiber bundle. The longer the fiber tracking, the better integrity and connectivity of a real nerve bundle. Importantly, all these findings were in agreement with histopathological findings of CSM, including axon damage and/or demyelination [35].

There are several limitations of our study. First, we used relatively thicker axial slices (7 mm) for diffusion MR imaging when compared with the previous studies (3 or 5 mm). The gap of 2.2 mm adopted between slices would lead to loss of information during the process of

three-dimensional reconstruction of fiber tractography. Further, we only used a single orientation for one voxel in fiber tractography, resulting in a potential for incorrect (false positive) or ineffective tracking (false negative) in voxels with more than one orientation of fiber bundles. Finally, CSM is a result of age-related degeneration of the cervical spine with abnormal curvature in elderly persons. However, for the small number of the subjects recruited in our study, the age of healthy subjects (42 years) was younger than in the patient group (approximately 56 years). Further, the subjects showed disparity in cervical spine curvature (HS: 10.1-18.5; HC: 20.4-30.4; CSM: 42.4-44.47). Thus, these potentially confounding factors should be controlled in a future large-scale population study.

In summary, we introduced a reliable quantitative analysis approach for diffusion tensor fiber tractography to delineate the extent and severity of spinal tract damages in CSM. We also identified the confounding factors, i.e. ROI selection and curvature of cervical spine, which could affect the outcome of the quantitative FT analyses for CSM patients.

References

1. **McCormick, W.E., M.P. Steinmetz, and E.C. Benzel, *Cervical spondylotic myelopathy: make the difficult diagnosis, then refer for surgery.* Cleve Clin J Med, 2003. 70(10): p. 899-904.**
2. **Ichihara, K., et al., *Mechanism of the spinal cord injury and the cervical spondylotic myelopathy: new approach based on the mechanical features of the spinal cord white and gray matter.* J Neurosurg, 2003. 99(3 Suppl): p. 278-285.**
3. **Rao, R., *Neck Pain, Cervical Radiculopathy, and Cervical Myelopathy: Pathophysiology, Natural History, and Clinical Evaluation.* The Journal of Bone & Joint Surgery, 2002. 84(10): p. 1872-1881.**
4. **Baron, E.M. and W.F. Young, *Cervical spondylotic myelopathy: a brief review of its pathophysiology, clinical course, and diagnosis.* Neurosurgery, 2007. 60(1 Supp1 1): p. S35-41.**
5. **Matsumoto, M., et al., *Increased signal intensity of the spinal cord on magnetic resonance images in cervical compressive myelopathy. Does it predict the outcome of conservative treatment?* Spine (Phila Pa 1976), 2000. 25(6): p. 677-82.**
6. **Bednarik, J., et al., *Presymptomatic spondylotic cervical myelopathy: an update predictive model.* Eur Spine J, 2008. 17: p. 421-431.**
7. **Kadanka, Z., et al., *Cross-sectional Transverse Area and Hyperintensities on Magnetic Resonance Imaging in Relation to the Clinical Picture in Cervical Spondylotic Myelopathy.* Spine, 2007. 32(23): p. 2573-2577.**
8. **Baptiste, D.C. and M.G. Fehlings, *Pathophysiology of cervical myelopathy.* The Spine Journal, 2006. 6: p. 190S-197S.**
9. **Facon, D., et al., *MR Diffusion Tensor Imaging and Fiber Tracking in Spinal Cord Compression.* Am J Neuroradiol, 2005. 26: p. 1587-1594.**
10. **Demir, A., et al., *Diffusion-weighted MR imaging with apparent diffusion coefficient and apparent diffusion tensor maps in cervical spondylotic myelopathy.* Radiology, 2003. 229(1): p. 37-43.**
11. **Mamata, H., F.A. Jolesz, and S.E. Maier, *Apparent diffusion coefficient and fractional anisotropy in spinal cord: age and cervical spondylosis-related changes.* J Magn Reson Imaging, 2005. 22(1): p. 38-43.**
12. **Xiangshui, M., et al., *3 T magnetic resonance diffusion tensor imaging and fibre tracking in cervical myelopathy.* Clin Radiol, 2010. 65(6): p. 465-73.**
13. **Chang, Y., et al., *Diffusion Tensor Imaging and Fiber Tractography of Patients with Cervical Spinal Cord Injury.* J Neurotrauma, 2010.**
14. **Budzik, J.F., et al., *Diffusion tensor imaging and fibre tracking in cervical spondylotic myelopathy.* Eur Radiol, 2010.**
15. **Song, T., et al., *Diffusion tensor imaging in the cervical spinal cord.* Eur Spine J, 2010.**
16. **Voss, H.U., et al., *Diffusion Tensor Imaging in Cervical Spondylotic Myelopathy.* World Spine Journal, 2007. 2(3): p. 140-147.**
17. **Shanmuganathan, K., et al., *Diffusion tensor MR imaging in cervical spine trauma.* AJNR Am J Neuroradiol, 2008. 29(4): p. 655-9.**

18. **Lee, J.W., et al.,** ***Diffusion tensor imaging and fiber tractography in cervical compressive myelopathy: preliminary results.*** **Skeletal Radiol, 2011. 40(12): p. 1543-51.**
19. **Nakamura, M., et al.,** ***Clinical significance of diffusion tensor tractography as a predictor of functional recovery after laminoplasty in patients with cervical compressive myelopathy.*** **J Neurosurg Spine, 2012. 17(2): p. 147-52.**
20. **Chang, Y., et al.,** ***Diffusion tensor imaging and fiber tractography of patients with cervical spinal cord injury.*** **J Neurotrauma, 2010. 27(11): p. 2033-40.**
21. **Basser, P.J. and D.K. Jones,** ***Diffusion-tensor MRI: theory, experimental design and data analysis - a technical review.*** **NMR in Biomedicine, 2002. 15: p. 456-467.**
22. **Mori, S. and P.C. van Zijl,** ***Fiber tracking: principles and strategies - a technical review.*** **NMR in biomedicine, 2002. 15(7-8): p. 468-80.**
23. **Facon, D., et al.,** ***MR diffusion tensor imaging and fiber tracking in spinal cord compression.*** **AJNR. American journal of neuroradiology, 2005. 26(6): p. 1587-94.**
24. **Xiangshui, M., et al.,** ***3 T magnetic resonance diffusion tensor imaging and fibre tracking in cervical myelopathy.*** **Clinical radiology, 2010. 65(6): p. 465-73.**
25. **Budzik, J.F., et al.,** ***Diffusion tensor imaging and fibre tracking in cervical spondylotic myelopathy.*** **European radiology, 2011. 21(2): p. 426-33.**
26. **Budzik, J.F., et al.,** ***Diffusion tensor imaging and fibre tracking in cervical spondylotic myelopathy.*** **Eur Radiol, 2011. 21(2): p. 426-33.**
27. **Flint, J.J., et al.,** ***Cellular-level diffusion tensor microscopy and fiber tracking in mammalian nervous tissue with direct histological correlation.*** **NeuroImage, 2010. 52(2): p. 556-61.**
28. **Chang, Y., et al.,** ***Diffusion tensor imaging and fiber tractography of patients with cervical spinal cord injury.*** **Journal of neurotrauma, 2010. 27(11): p. 2033-40.**
29. **Morgan, P.S., et al.,** ***Correction of spatial distortion in EPI due to inhomogeneous static magnetic fields using the reversed gradient method.*** **J Magn Reson Imaging, 2004. 19(4): p. 499-507.**
30. **Chuang, T.C., et al.,** ***PROPELLER-EPI with parallel imaging using a circularly symmetric phased-array RF coil at 3.0 T: application to high-resolution diffusion tensor imaging.*** **Magn Reson Med, 2006. 56(6): p. 1352-8.**
31. **Andersson, J.L., S. Skare, and J. Ashburner,** ***How to correct susceptibility distortions in spin-echo echo-planar images: application to diffusion tensor imaging.*** **NeuroImage, 2003. 20(2): p. 870-88.**
32. **Cui, J.L., et al.,** ***Entropy-based analysis for diffusion anisotropy mapping of healthy and myelopathic spinal cord.*** **Neuroimage, 2011. 54(3): p. 2125-31.**
33. **Cui, J.L., et al.,** ***Orientation entropy analysis of diffusion tensor in healthy and myelopathic spinal cord.*** **Neuroimage, 2011. 58(4): p. 1028-33.**
34. **Ciccarelli, O., et al.,** ***Spinal cord spectroscopy and diffusion-based tractography to assess acute disability in multiple sclerosis.*** **Brain : a journal of neurology, 2007. 130(Pt 8): p. 2220-31.**
35. **Beaulieu, C., et al.,** ***Changes in water diffusion due to Wallerian degeneration in peripheral nerve.*** **Magnetic resonance in medicine : official journal of the Society of Magnetic Resonance in Medicine / Society of Magnetic Resonance in Medicine, 1996. 36(4): p. 627-31.**

Table(s) in MS Word

Table 1 Summary of clinical and radiological evaluations of cervical spondylotic myelopathy patients

Cases		1	2	3	4	5	6	7
Age		45	57	46	57	67	56	62
Gender		M	F	M	F	M	F	F
Diagnosis		CSM	CSM	CSM	CSM	CSM	CSM	CSM
Clinical signs	Hoffman Sign	+	-	+	+	+	+	+
	Finger Escape	4	0	1	2	0	0	2
	Babinski Sign	+	+	-	+	N.T.	-	+
	Ankle Clonus	-	+	-	-	+	-	-
mJOA score	mJOAsum	7.5	13	11	11	13	11	10
	mJOAmotion	3	5	6	5	5.5	6	2
	mJOA sensory	1.5	5	3	5	5	4.5	5
	mJOA bladder	3	3	2	1	3	1	3
	mJOA upperlimb	1	6	4	4	4	2.5	2.5
	mJOA lowerlimb	3	2.5	4	4	4.5	6	2.5
MRI	Offending Levels	c3/4	c5/6	c4/5	c5/6, 6/7	c4/5, 5/6	c3/4, 4/5, 5/6, 6/7	c3/4,4/5,5/6
	Maximal compression level	c3/4	c5/6	c4/5	c5/6	c4/5	c3/4	c5/6
	T2 HSI	-	-	+	-	+	+	-
SEP	Amplitude	decreased	normal	decreased	normal	normal	normal	decreased
	Latency	prolonged	normal	normal	normal	normal	normal	prolonged

Figure1

Click here to download high resolution image

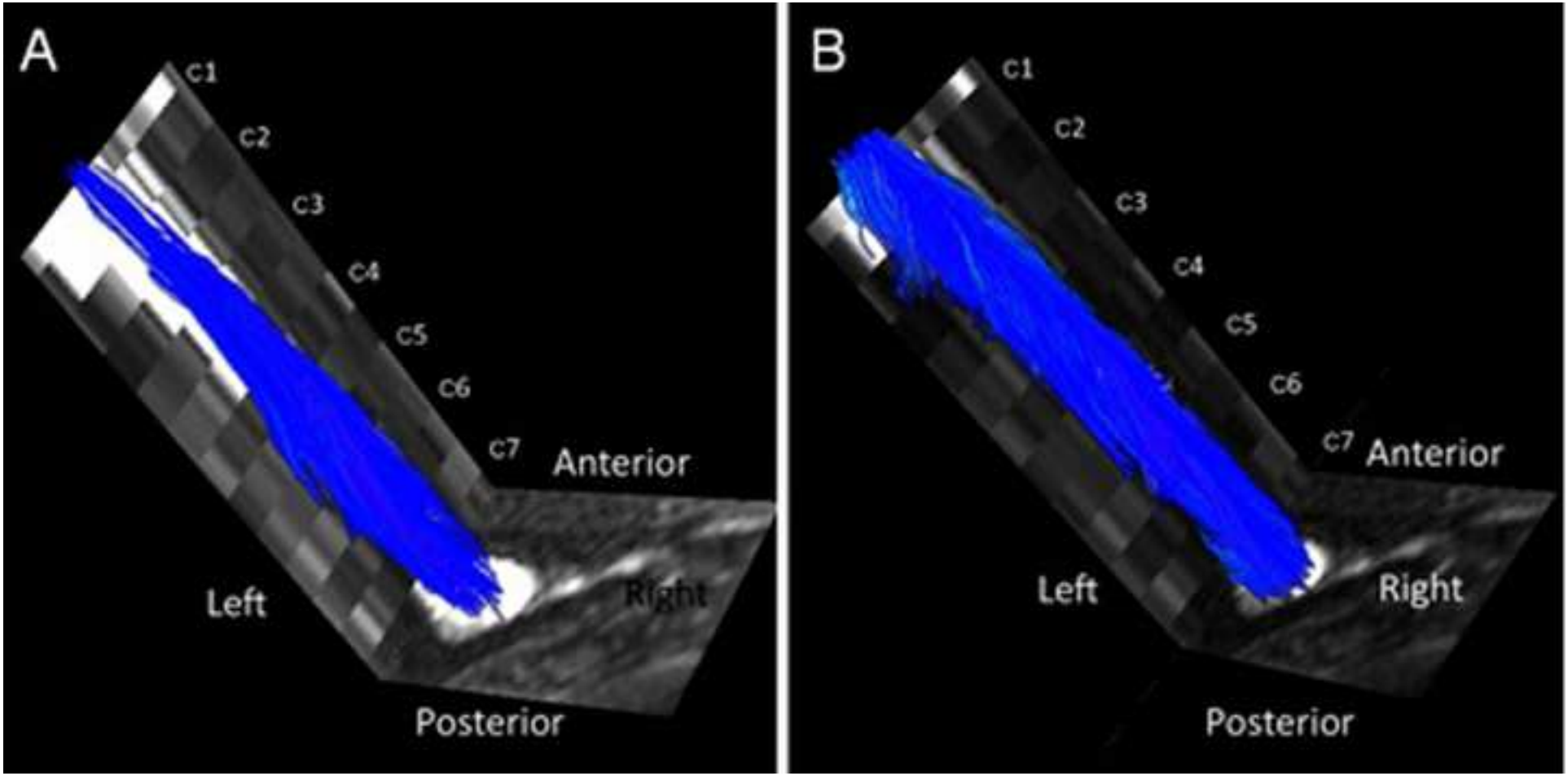

Figure2

Click here to download high resolution image

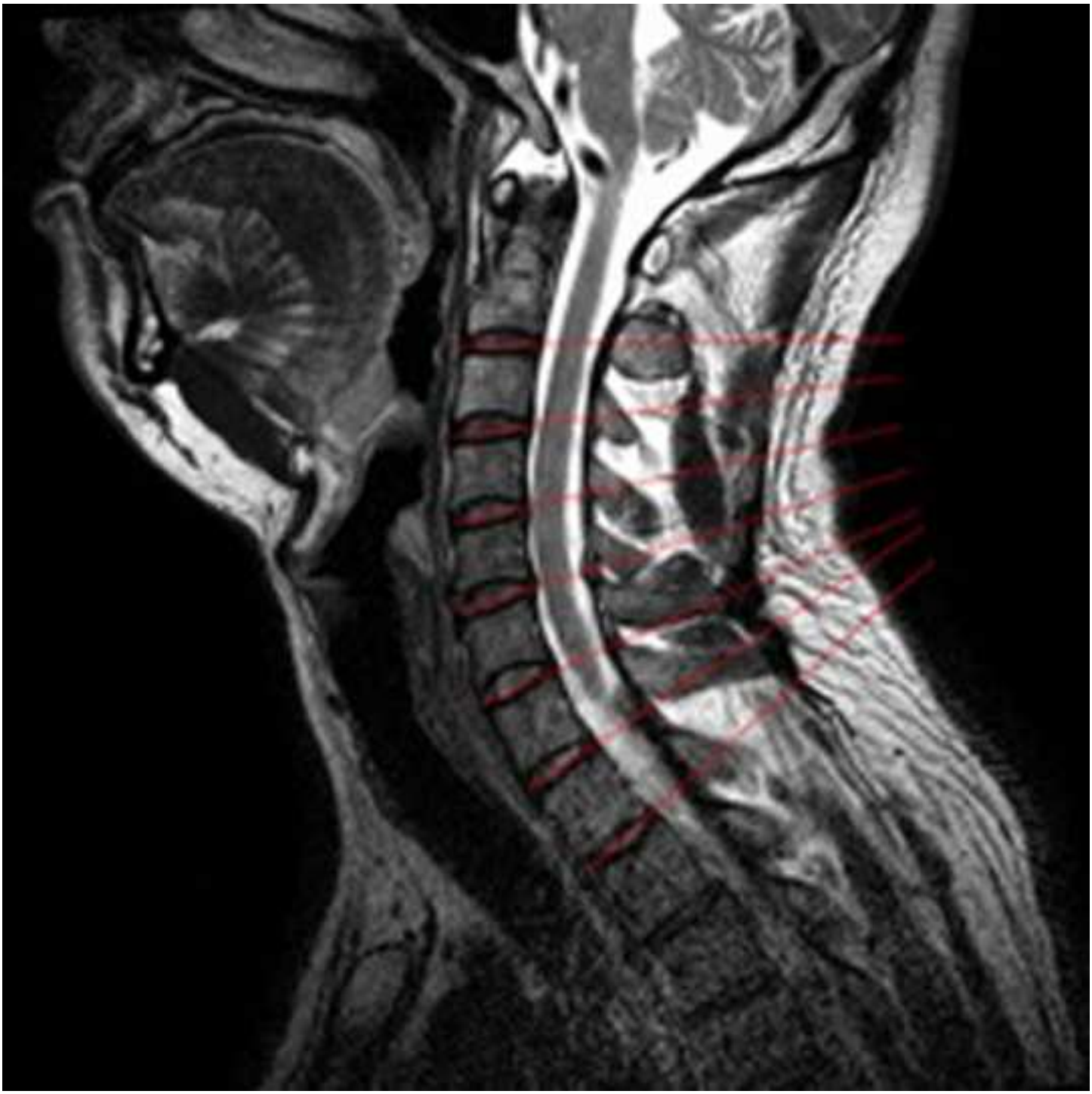

Figure3

Click here to download high resolution image

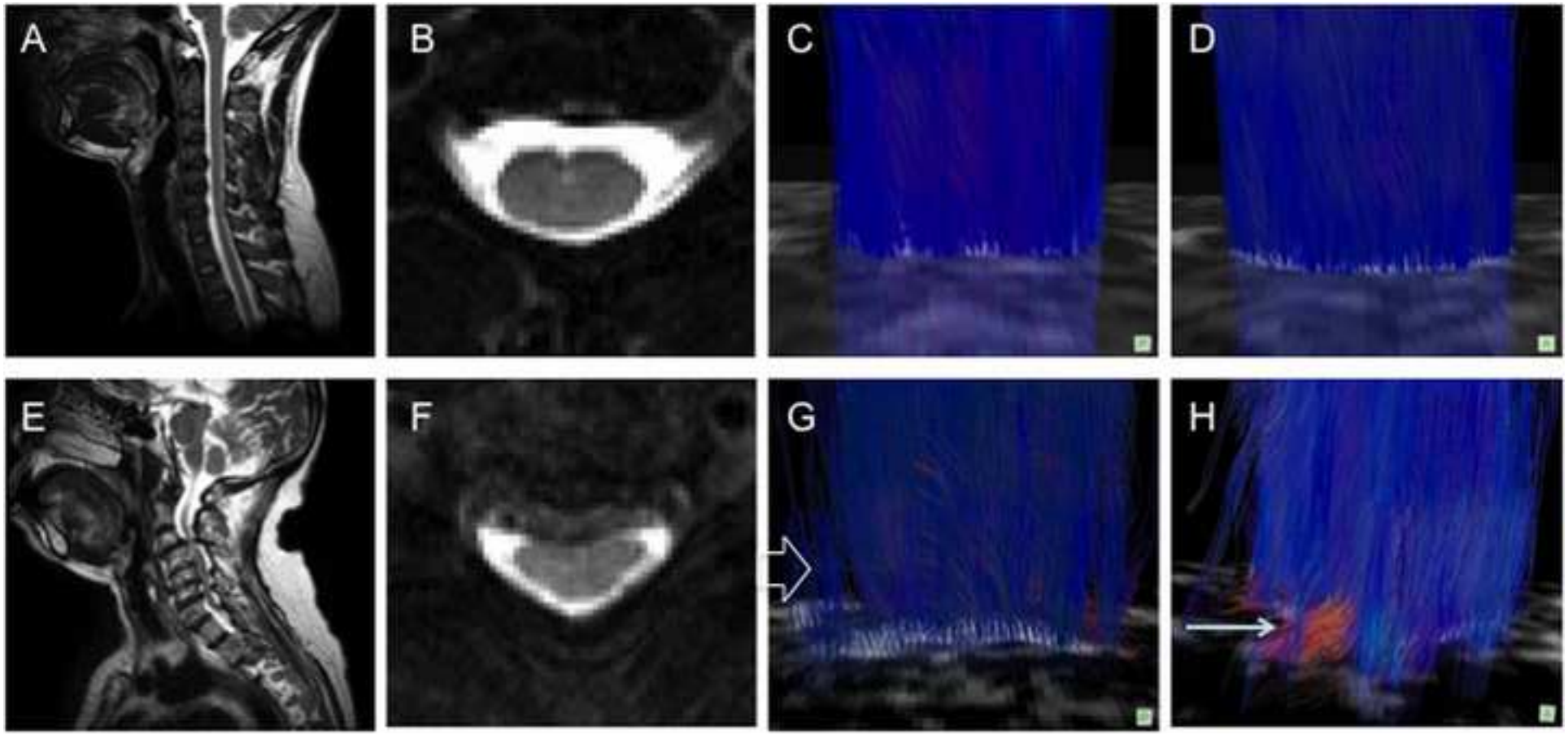

Figure4

Click here to download high resolution image

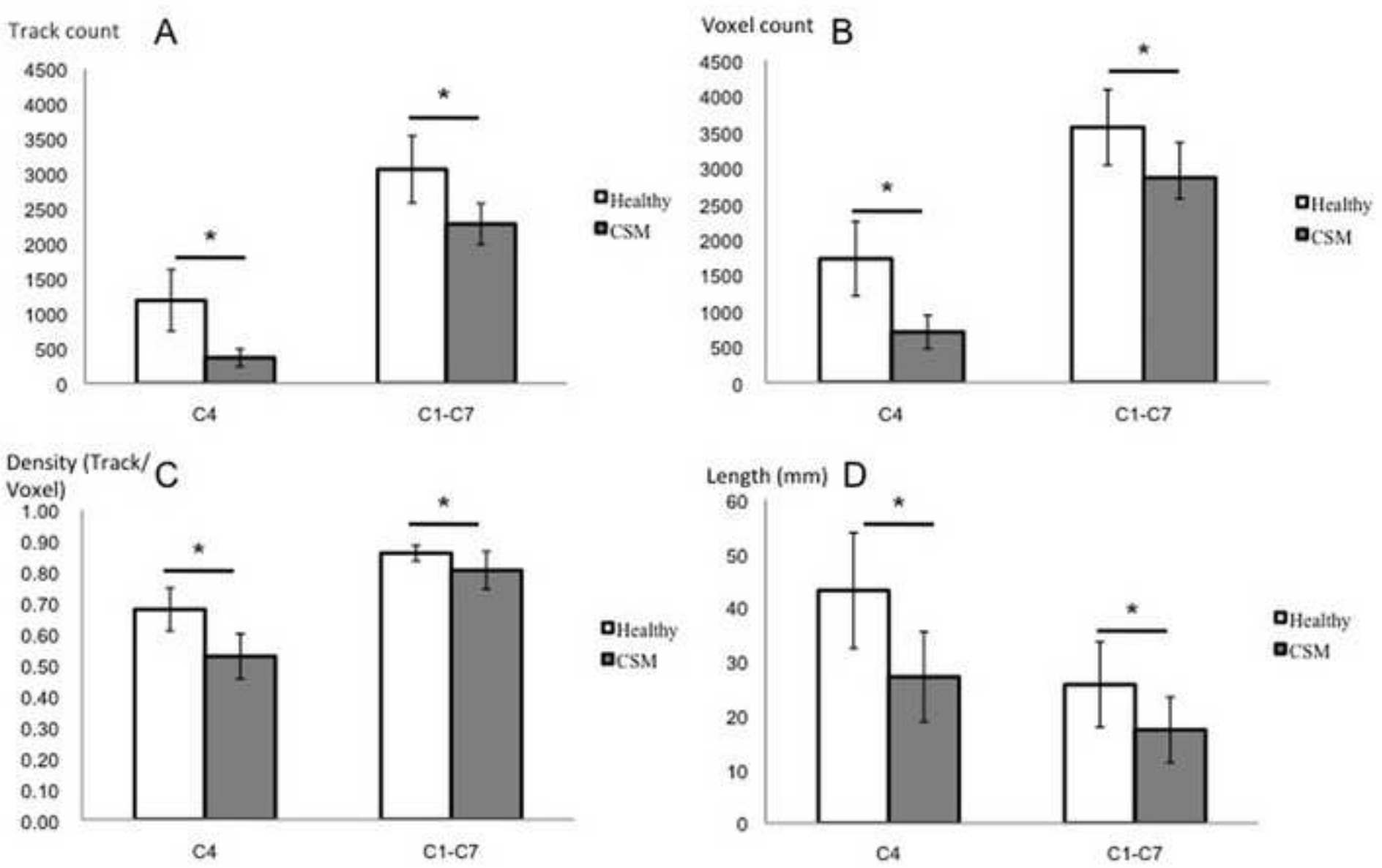

Figure5

Click here to download high resolution image

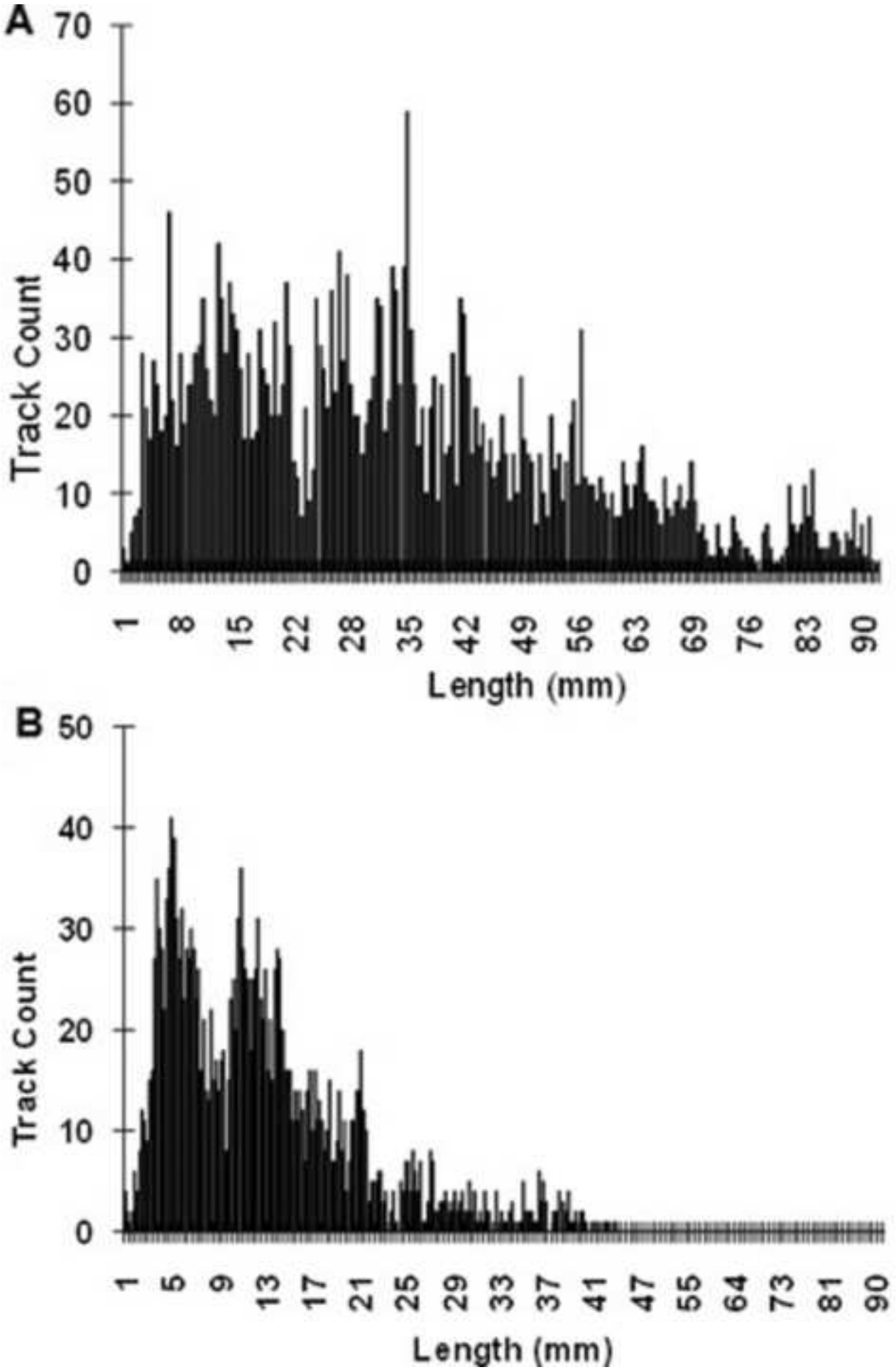

Figure6

Click here to download high resolution image